The Breast 62 (2022) 152–161

Contents lists available at ScienceDirect

The Breast

journal homepage: www.journals.elsevier.com/the-breast

Essential amino acids deprivation is a potential strategy for breast cancer treatment

Yajie Zhao, Chunrui Pu, Zhenzhen Liu *

Department of Breast Cancer Center, Affiliated Cancer Hospital of Zhengzhou University, Henan Cancer Hospital, 127 Dongming Road, Zhengzhou, 450008, China

ARTICLE INFO

Keywords:
Breast cancer
Essential amino acid
Metabolic reprogramming
PD-L1
Tregs

ABSTRACT

Aims: The study aimed to search novel, simple and practical index reflecting the level of essential amino acids (EAAs) metabolism in breast cancer (BC), as well as to explore the effect of enhanced EAAs metabolism on the prognosis and immune microenvironment of BC, thus providing new evidence for the application of EAAs deprivation in the BC treatment.

Methods: The study includes the analysis of multi-omics and clinical data of 13 BC cell lines and 2898 BC patients in the public database. Further validation was performed using multi-omics and immunohistochemistry data from 83 BC tissue samples collected at our hospital.

Results: According to the multi-omics data, the SLC7A5 to SLC7A8 Ratio (SSR) score was found to be significantly correlated with the EAAs level and EAAs-metabolic activity of BC, suggesting that the SSR score might be used as a biomarker to assess the degree of EAAs metabolism in BC. Besides, BC patients with high EAAs metabolism had shorter overall survival (OS) time, higher PD-L1 expression, and higher T regulatory cells (Tregs) infiltration, indicating that a high EAAs metabolism was related to a poor prognosis and immune suppression in BC. Additionally, MYC amplification is a critical molecular process in the metabolic reprogramming of EAAs in BC.

Conclusion: EAAs may be a possible therapeutic target for BC treatment.

1. Introduction

Breast cancer (BC) has surpassed all other types of cancer in terms of incidence [1]. Although standard treatment has considerably improved BC prognosis, many patients with drug resistance and relapse remain optimistic for the development of more comprehensive treatment techniques. In recent decades, tumor metabolism has gotten a lot of attention in cancer research. An emerging therapeutic method for cancer treatment is to target altered tumor metabolism [2,3]. Given these facts, targeting tumor metabolism could open up new avenues for BC treatment.

Rapid proliferation is a characteristic of tumor cells. To meet the needs of rapid proliferation, BC cells need to uptake a large number of EAAs. Du et al. [4]. Have demonstrated that EAAs uptake in BC cells is significantly higher than in normal breast cells. Furthermore, oncogenic genes can modify BC cells' metabolic pathways, making them more dependent on exogenous EAAs for survival. Lien et al. [5]. observed that the proliferation of BC cells with oncogenic PI3K is impaired in growth media in which methionine is replaced by homocysteine, such that oncogenic PI3K promotes methionine dependency in BC cells.

EAAs not only provide important raw materials for BC cell protein synthesis but also affect the biological behavior of BC cells and cause therapeutic resistance. Cancer stem cells (CSCs) are one of the major causes of tumor recurrence and treatment resistance in BC [6]. Elena et al. [7]. found that methionine plays a critical role in maintaining the self-renewal and survival of CSC. Methionine restriction reduced the CSC population in TNBC. Besides, Saito et al. [8]. found that leucine not only promotes the proliferation of ER + BC cells but also participates in the mechanism of resistance to tamoxifen in ER + BC. In addition, EAAs, as important nutrients, mediate the development of the immunosuppressive tumor microenvironment in BC. For example, kynurenine, a product of tryptophan metabolism, can inhibit the proliferation and differentiation of T cells, which leads to immune escape and tumor progression of BC [9–11]. These findings reveal the intrinsic relationship between EAAs metabolism and the immune microenvironment in BC.

BC cells were more strictly dependent on the supply of exogenous essential amino acids, emphasizing the value of EAAs deprivation therapy. Blocking off the supply of exogenous EAAs to BC cells will cause amino acid starvation, growth arrest, and apoptosis [12]. According to preclinical experiments, methionine deprivation inhibits TNBC cell migration and invasion, as well as the growth of tumor nodules in the

* Corresponding author.
E-mail address: zlyyliuzhenzhen0800@zzu.edu.cn (Z. Liu).

https://doi.org/10.1016/j.breast.2022.02.009
Received 6 November 2021; Received in revised form 14 February 2022; Accepted 16 February 2022
Available online 20 February 2022

Abbreviations

BC	Breast cancer
EAA	Essential amino acid
TCGA	The Cancer Genome Atlas
CCLE	Cancer Cell Line Encyclopedia
METABRIC	Molecular Taxonomy of Breast Cancer International Consortium
CNV	Copy number variation
GSEA	Gene Set Enrichment Analysis
HR	Hazard ratio
CI	Confidence interval
SSR	SLC7A5 to SLC7A8 Ratio
TME	Tumor microenvironment
Tregs	T regulatory cells

lungs of mice [13]. Besides, methionine deprivation could enhance the sensitivity of TNBC cells to TRAIL-R2 targeted therapies, such as lexatumumab, and augment their antitumor activity in vivo [14]. These preclinical results suggest that EAAs deprivation may be a new strategy for breast cancer therapy.

Although preclinical animal models have confirmed that EAAs metabolism can promote BC progression and the development of the immunosuppressive tumor microenvironment, there is still a lack of relevant clinical evidence. In this study, we first proposed a novel biomarker to reflect the EAAs metabolism level of BC patients. In this view, we further analyzed the effects of EAAs metabolism on the prognosis and tumor immune microenvironment of BC patients. These findings will provide a new theoretical basis for the application of EAAs deprivation in the treatment of BC.

2. Materials and methods

2.1. BC patients and cell lines

The RNA-seq data and metabolomic data in thirteen BC cell lines were downloaded from Cancer Cell Line Encyclopedia (CCLE) [15]. Besides, we analyzed 2898 BC samples from The Cancer Genome Atlas (TCGA, n = 994) and Molecular Taxonomy of Breast Cancer International Consortium (METABRIC, n = 1904) databases, whose clinical information, RNA-seq data, and copy number variation (CNV) data were obtained from cBioPortal (https://www.cbioportal.org/). We also enrolled the RNA-seq, proteomics, metabolomics, and pathology data (HNCH-BC) from 83 BC patients treated in our hospital (Table 1). This study was approved by the ethics committee of the Affiliated Cancer Hospital of Zhengzhou University (Zhengzhou, China) (HNCH-BC006), and informed consent was obtained from the 83 BC patients. The ComBat function of sva package-R was used to eliminate the batch effects.

2.2. SSR score and EAAs metabolism

2.2.1. Calculation of SSR score

The SSR score was a SLC7A5 to SLC7A8 ratio, which could be calculated using the mRNA expression value or protein level of two genes.

2.2.2. Correlation between SSR score and the level of EAAs in BC cell lines

Based on the RNA-seq data of BC cell lines, SSR was computed by dividing the mRNA expression value of SLC7A5 by the mRNA expression value of SLC7A8. The levels of nine EAAs were obtained from metabolomic data of thirteen BC cell lines (Supplementary Table 1). Pearson's correlation analysis was employed to evaluate the correlation between the SSR score and the level of EAAs; a *p-value* < 0.05 was considered the significance threshold.

Table 1
Clinical characteristics of breast cancer patients.

Characteristics	METABRIC	TCGA	HNCH-BC
	n = 1904	n = 994	n = 83
Age (year)	61.09 ± 0.29	58.30 ± 0.42	50.41 ± 1.09
Molecular subtype			
Luminal A	760(39.91%)	499(50.2%)	36(43.37%)
Luminal B	617(32.41%)	197(19.82%)	17(20.48%)
Her-2	231(12.13%)	114(11.47%)	20(24.1%)
Triple-negative	296(15.55%)	171(17.2%)	10(12.05%)
Uncertain	0(0%)	13(1.31%)	0(0%)
T stage (8th AJCC)			
T1	821(43.12%)	255(25.65%)	28(33.73%)
T2	968(50.84%)	586(58.95%)	45(54.22%)
T3	95(4.99%)	113(11.37%)	10(12.05%)
T4	0(0%)	37(3.72%)	0(0%)
Uncertain	20(1.05%)	3(0.31%)	0(0%)
N stage (8th AJCC)			
N0	993(52.15%)	473(47.59%)	43(51.81%)
N1	604(31.72%)	326(32.79%)	28(33.73%)
N2	204(10.72%)	113(11.37%)	10(12.05%)
N3	103(5.41%)	63(6.34%)	2(2.41%)
Uncertain	0(0%)	19(1.91%)	0(0%)
M stage (8th AJCC)			
M0	1875(98.48%)	962(96.78%)	83(100%)
M1	9(0.47%)	20(2.01%)	0(0%)
Uncertain	20(1.05%)	12(1.21%)	0(0%)
Stage (8th AJCC)			
Stage I	573(30.09%)	166(16.7%)	27(32.53%)
Stage II	1091(57.3%)	575(57.85%)	42(50.6%)
Stage III	213(11.19%)	218(21.93%)	14(16.87%)
Stage IV	9(0.47%)	20(2.01%)	0(0%)
Uncertain	18(0.95%)	15(1.51%)	0(0%)

AJCC: American Joint Committee on Cancer.

2.2.3. Correlation between SSR score and the level of EAAs in BC tissue

The HNCH-BC database was used to acquire RNA-seq, proteomic, and metabolomic data from 24 BC patients (24 normal tissue samples and 24 BC samples). SSR scores were determined at the mRNA and protein levels using the BC sample's RNA-seq and proteomic data. The levels of nine EAAs were obtained from metabolomic data of 24 BC samples (Supplementary Table 2 and 3). Correlation between the level of nine EAAs and SSR scores in BC tissues was evaluated by using Pearson's correlation analysis.

Multi-omics analysis was performed at Applied Protein Technology Co., Ltd (Shanghai, China). Sequencing was performed using the Next-Generation Sequencing (NGS) technology based on an Illumina Hiseq platform. The study of free amino acids and their derivatives was performed using a liquid chromatography-tandem mass spectrometry (LC-MS/MS) system. A UHPLC (1290 Infinity LC, Agilent Technologies) coupled to a QTRAP (AB SCIEX 5500) was used to separate amino acids with greater efficiency. A quantitative proteomic analysis was performed via tandem mass tag (TMT) technology. Tandem mass spectrometry (TMS) spectral data were obtained from the MASCOT engine (Matrix Science, London, UK; version 2.2) embedded into Proteome Discoverer 1.4 software.

2.2.4. Gene set enrichment analysis (GSEA)

In this study, gene set enrichment analysis (GSEA) was carried out to elucidate the difference of EAAs metabolism between high- and low-SSR groups. Metabolism-related genes of nine EAAs were obtained from the MSigDB database (https://www.Gsea-msigdb.org/gsea/msigdb/), and integrated into one gene set named "EAAs metabolism" (Supplementary Table 4). EAAs metabolism was used for the gene set file (.gmt). The value of SSR was used as a phenotype label (.cls). BC patients were divided into high- and low-SSR groups according to the value of SSR

(divided by median value [16,17]). As an expression dataset file, we used BC RNA-seq data from TCGA and METABRIC (.gct). The GSEA software (version 3.0) was used to create and load all expression datasets (.gct), phenotype label (.cls), and gene set (.gmt) files. The GSEA was performed in accordance with its user manual (http://software.broadinstitute.org/gsea/doc/GSEAUserGuideFrame.html). To acquire a normalized enrichment score (NES), the number of gene set permutations was set at 1000 for each analysis. The nominal p-value <0.05, |NES|>1, and False Discovery Rate (FDR) < 0.05 were considered to indicate significant enrichment results.

2.3. Cut-off value of SSR scores

BC patients from METABRIC were used as a training set to explore the relationship between SSR and survival. Two tools, the Cutoff Finder tool, and the X-tile program were used to evaluate the optimal cut-off value of SSR. Cutoff Finder [18] is an online collection of optimization and visualization methods (http://molpath.charite.de/cutoff) for cutoff determination. This method fits Cox proportional hazard models to the dichotomized variable and the survival variable. X-tile program [19] is also a freely available tool that is specialized in the analysis of survival data and uses a minimal p-value approach for cutoff optimization (http://www.tissuearray.org/rimmlab/). Moreover, 0.9628 was consistently recommended by two methods as the optimal cut-off value of SSR in BC patients from METABRIC, which with the most significant overall survival split and with a minimal p-value.

2.4. Regulatory T cells (Tregs) infiltration and programmed Death-Ligand 1(PD-L1) expression

2.4.1. Tregs infiltration and PD-L1 expression in TCGA and METABRIC database

CIBERSORT (https://cibersort.stanford.edu/) deconvolution algorithm, by which the normalized gene expression matrix can be transformed into the composition of infiltrating immune cells. During the CIBERSORT, the abundance of Tregs infiltration in BC samples from TCGA and METABRIC was calculated. Differential abundance of Tregs infiltration between BC subgroups was assessed using Wilcoxon tests and $p < 0.05$ was the significance threshold.

PD-L1 expression levels of BC samples were obtained from RNA-seq data in TCGA and METABRIC. The differential expression level of PD-L1 between BC subgroups was assessed using Wilcoxon tests and $p < 0.05$ was the significance threshold.

2.4.2. Validation of tregs infiltration and PD-L1 in HNCH-BC database

The HNCH-BC database was used to further validate the above results from the public database by using the RNA-seq and pathology data of 59 BC patients. Quantification of the Tregs infiltrate in 59 BC tumor biopsies from the HNCH-BC database was performed using m-IHC labeling and digital image analysis. Quantification of Tregs (Foxp3+) was separately identified within the stromal and intra-tumoral areas. Intratumoral Tregs were defined as Tregs within cancer cell nests and in direct contact with tumor cells. Similarly, stromal Tregs are defined as Tregs within the tumor stroma and not in direct contact with tumor cells. Primary antibodies including m-IHC staining: anti-CD8 (clone SP16), anti-CD4 (clone EP204), and anti-Foxp3 (clone 236A/E7) were obtained from ZSGB-BIO (Beijing, China). Differential abundance of Tregs and Treg subpopulations between BC subgroups were assessed using Wilcoxon tests. p-value < 0.05 was considered as the significance threshold.

Quantification of PD-L1 positive cells in 59 BC tumor biopsies from the HNCH-BC database was performed using m-IHC labeling and digital image analysis. Primary antibodies including m-IHC staining: anti-PD-L1 (clone SP142) was obtained from ZSGB-BIO, Beijing, China. Differential percentage and density of PD-L1 positive cells between BC subgroups were assessed using Wilcoxon tests. p-value < 0.05 was considered as the significance threshold.

Positive cells were defined as cells with true immunofluorescence signal detected and with the right expression pattern. More than 12 fields per slide were selected to calculate the number, percentage, and density of positive cells under the 200 × magnification. The stained slides were scanned using the PerkinElmer Vectra and analyzed by inForm Advanced Image Analysis software (PerkinElmer, Massachusetts, USA).

2.5. Association between MYC CNV and SSR score

The MYC CNV data of BC patients in the TCGA and METABRIC database were obtained from cBioPortal (https://www.cbioportal.org/). Wilcoxon tests were employed to compare SSR scores, SLC7A5 and SLC7A8 between BC patients with different MYC CNV statuses. p-value < 0.05 was considered as the significance threshold.

2.6. Statistical analysis

GraphPad Prism and R packages were used for all statistical analyses. To investigate correlations between variables, Pearson's correlation analysis was used. Wilcoxon test was employed to analyze continuous variables between two groups. Paired t-test was used for matched data. To compare survival outcomes, Kaplan-Meier curves and log-rank tests were utilized. The TCGA and METABRIC databases were used to compile survival data. Multivariate Cox proportional hazard regression models were used to calculate hazard ratios (HRs) with 95% confidence intervals (CIs). Models were adjusted for prognostic clinical covariates. A two-tailed $p < 0.05$ was the significance threshold for this study.

3. Result

3.1. The SSR score serves as a biomarker for EAA metabolism in BC

The link between SSR score and EAAs was investigated using RNA-seq and metabolomic data from 13 BC cell lines. We performed pearson's correlation analysis to determine the relationship between SSR scores and the levels of EAAs in BC cell lines. The obtained data showed a significant correlation between SSR score and nine EAAs (Ile: $R = 0.75$, $p = 0.0029$; Leu: $R = 0.75$, $p = 0.0034$; Lys: $R = 0.67$, $p = 0.012$; Met: $R = 0.76$, $p = 0.0028$; Phe: $R = 0.76$, $p = 0.0028$; Thr: $R = 0.51$, $p = 0.076$; Trp: $R = 0.69$, $p = 0.0093$; Tyr: $R = 0.62$, $p = 0.025$; Val: $R = 0.72$, $p = 0.006$), implying that SSR can roughly reflect the level of EAA uptake and incorporation in BC cell lines (Fig. 1A).

To further verify the correlation between the SSR score and the level of nine EAAs in BC tumor tissue, we analyzed transcriptomic, proteomic, and metabolomic data from 24 BC patients, and the SSR score was computed at the mRNA and protein level, respectively. The correlation between the SSR score and the levels of nine EAAs in BC tumor tissue was investigated using Pearson's correlation analysis. The obtained data revealed that the SSR score was consistently linked with the levels of nine EAAs in BC tumor tissue at the mRNA or protein level (Fig. 1C) (all $p < 0.05$), implying that SSR can also reflect EAA levels in BC samples.

To study the variations in EAAs metabolic activity in BC patients with different SSR scores, we estimated the SSR scores of 2898 BC patients from TCGA and METABRIC, and then GSEA was carried out to elucidate the variations in EAAs metabolism between high-and low-SSR score samples (divided by median value). The EAAs metabolism pathway was consistently upregulated in high-SSR samples (METABRIC: NES = 1.57, FDR = 0.004, $p = 0.004$; TCGA: NES = 1.56, FDR = 0.008, $p = 0.008$), implying that EAAs metabolism is more activated in high-SSR samples (Fig. 1D). Taken together, these findings show that the SSR score can be used as a biomarker to estimate the activity of EAA metabolism in BC samples.

Furthermore, we discovered that the level of EAAs and SSR score in BC tumor tissues were much higher than in corresponding normal tissues, indicating that BC tumor cells frequently uptake larger levels of

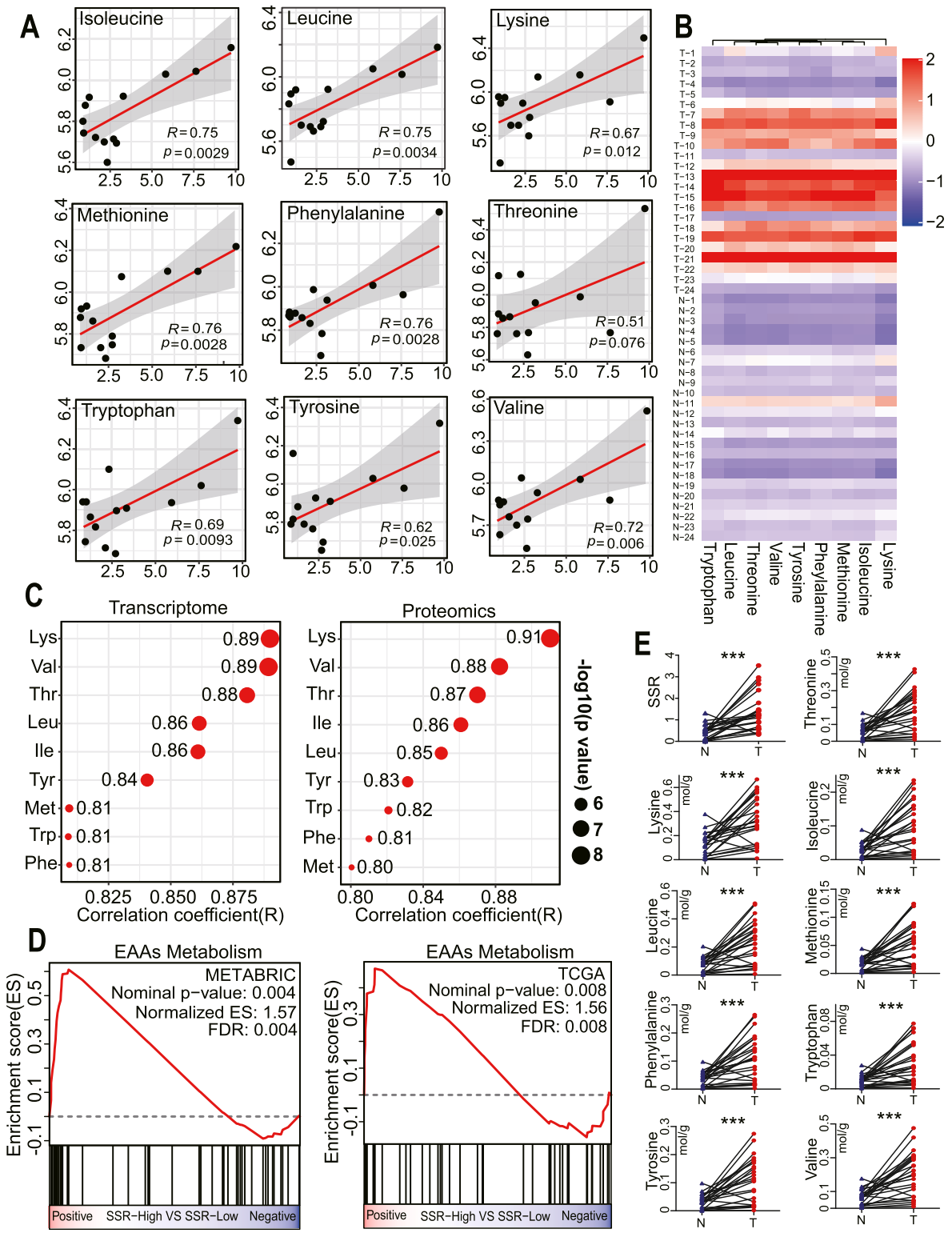

Fig. 1. The SSR score serves as a biomarker for EAA metabolism in BC, (A) Scatter plots indicating statistically significant correlations between the SSR score and the levels of nine EAAs in 13 BC cell lines. Pearson's correlation coefficient was used to determine the correlation coefficient. (B) Heatmap depicting the levels of nine EAAs in 24 BC tumor tissue and corresponding normal tissue samples. (C) Bubble chart highlighting the levels of nine EAAs in 24 BC tumor tissue were positively correlated with SSR score both in transcriptional (left) or translational level (right) (Met: Methionine, Lys: Lysine, VAL: Valine, Leu: Leucine, Ile: Isoleucine, Phe: Phenylalanine, Trp: Tryptophan, Thr: Threonine, Tyr: Tyrosine). The correlation coefficient was determined by Pearson's correlation. (D) GSEA plots demonstrate significantly increased EAA metabolism in high-SSR samples relative to low-SSR samples. (E) Variations SSR score and EAAs level between BC tumor tissue and corresponding normal tissue samples (Paired t-test; *** represent for $p < 0.001$)..

EAAs than normal cells (Fig. 1E, paired *t*-test, all $p < 0.001$). Importantly, the levels of EAAs in different BC tumor samples were also different, which indicates the metabolic heterogeneity of EAAs in BC patients. These results emphasize the necessity of exploring a biomarker to estimate the EAAs metabolic status of BC patients.

3.2. Effect of EAAs metabolism on survival of BC patients

To explore the relationship between EAAs metabolism and survival in BC patients, it is necessary to determine a cut-off point and to convert a continuous variable of SSR score into a dichotomization. We selected 1904 BC patients from the METABRIC database as the training set to find a cut-off point of SSR score, and the cut-off point determination was focused to optimize the correlation with survival. To optimize and validate the cut-off point, we used Cutoff Finder and X-tile. Finally, the optimal cutoff point was defined as 0.9628, with the most significant survival split and a minimal *p*-value (Fig. 2A–C).

The results of Kaplan-Meier survival analysis showed that BC patients with SSR>0.9628 was related to a worse prognosis in both the training and validation sets (METABRIC: HR = 1.245, 95% CI:1.107–1.402, median survival: 14.02 *vs* 11.02, $p = 0.0003$; TCGA: HR = 3.364, 95% CI:2.392–4.731, median survival: 17.69 *vs* 8.39, $p < 0.0001$) (Fig. 2D–E). Additionally, after adjusting for TNM stage and BC intrinsic subtypes, multivariate Cox proportional hazard models revealed that SSR>0.9628 was an independent predictor of a worse OS (METABRIC: HR = 1.222, 95% CI:1.085–1.376, $p = 0.001$; TCGA: HR = 6.701, 95% CI:4.281–10.487, $p < 0.001$) (Tables 2 and 3). These findings suggest that increased EAAs metabolism in BC patients has a statistically significant adverse effect on survival, and which was independent of BC intrinsic subtypes and tumor stage. Notably, we discovered a significant correlation between SSR scores and Ki-67, a cellular proliferation marker (METABRIC: $R = 0.51$, $p < 0.0001$; TCGA: $R = 0.49$, $p < 0.0001$) (Fig. 2F–G). As such, we speculate that differential proliferative activity may play a role in the predictive implications of SSR scores.

3.3. EAAs metabolism associated with immunosuppression in BC

EAAs are significantly reduced within the tumor microenvironment (TME) as a result of competition for nutrition by malignant and

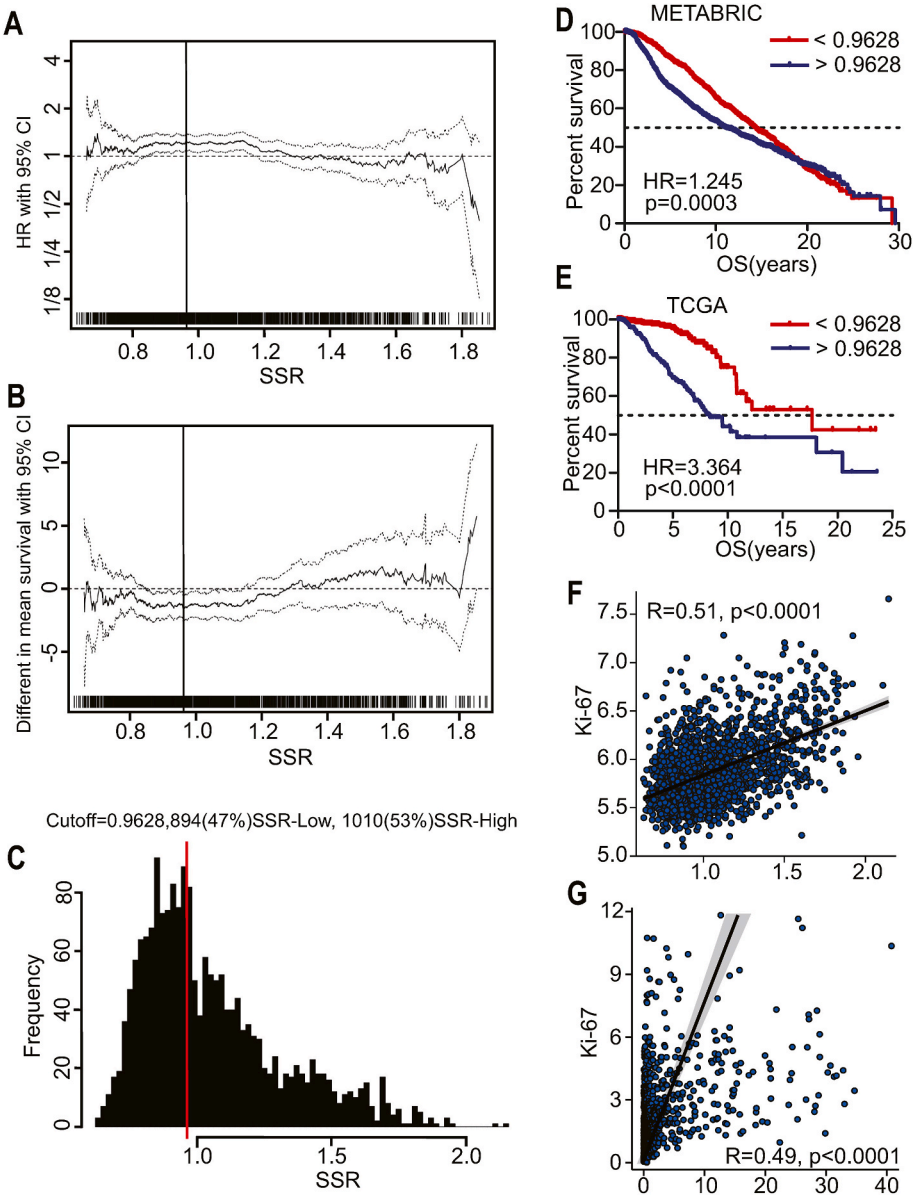

Fig. 2. Effect of EAAs metabolism on survival of BC patients, (A) SSR score was correlated with OS for each possible cutoff. The hazard ratio (HR) with a 95% CI is plotted in dependence on the cutoff. A vertical line designates the dichotomization showing the most significant correlation with survival. (B) The mean survival time is estimated for patients with high SSR scores and patients with low SSR values. The difference in the mean survival times is plotted. (C) Distribution of SSR scores in 1904 BC patients from METABRIC showing the optimal cutoff via vertical line. Kaplan-Meier curves comparing OS outcomes between BC patients with SSR>0.9628 and SSR<0.9628 in the training cohort (D) and validation cohort (E). The Log-rank test was used to examine the statistical significance of differences. Scatter plots show the significant correlations between SSR score and the level of Ki-67 in METABRIC (F) and TCGA (G), Pearson's correlation coefficient was used to determine the correlation coefficient.

Table 2
Multivariate Cox regression analyses of BC patients from METABRIC.

Factors	Hazard radio	95% CI	*p* value
TNM stage			<0.001
Stage I	1.000	Reference	
Stage II	1.807	1.546–2.112	<0.001
Stage III	2.029	1.687–2.441	<0.001
Stage IV	5.644	2.776–11.475	<0.001
PAM50 subtype			<0.001
Luminal A	1.000	Reference	
Luminal B	1.465	1.257–1.707	<0.001
Her-2	1.574	1.301–1.903	<0.001
Basal-like	1.373	1.129–1.675	<0.001
SSR score			0.001
SSR<0.9628	1.000	reference	
SSR>0.9628	1.222	1.085–1.376	0.001

Table 3
Multivariate Cox regression analyses of BC patients from TCGA.

Factors	Hazard radio	95% CI	*p* value
TNM stage			<0.001
Stage I	1.000	reference	
Stage II	1.382	0.901–1.998	0.021
Stage III	2.698	1.543–4.718	<0.001
Stage IV	10.834	4.973–23.603	<0.001
PAM50 subtype			<0.001
Luminal A	1.000	reference	
Luminal B	1.455	0.922–2.296	0.005
Her-2	2.248	1.257–4.019	<0.001
Basal-like	1.463	0.912–2.386	0.003
SSR score			<0.001
SSR<0.9628	1.000	reference	
SSR>0.9628	6.701	4.281–10.487	<0.001

immunological cells. This deficiency of EAAs can compromise immune cell function, hence inhibiting the anti-tumor immune response. Foxp3$^+$ regulatory T cells (Tregs) are the main immunosuppressive cell populations in TME. The CIBERSORT algorithm was used to gauge the Tregs infiltration in BC tumors. A higher percentage of Tregs infiltration was detected in BC patients with SSR>0.9628 (METABRIC: mean 1.35% *vs* 1.76%, $p = 0.0007$; TCGA: mean 1.96% *vs* 2.45%, $p = 0.0001$) (Fig. 3A–B).

To further verify the above results from RNA-seq, we employed an advanced multispectral imaging-based technology to quantify stromal (s-) and intra-tumoral (i-) Foxp3$^+$ Tregs separately. Consistently, a higher percentage and density of s-Foxp3$^+$ Tregs were detected in patients with SSR>0.9628 (cell density: mean 257.89 *vs* 391.77, $p = 0.021$; percentage: mean 7.76% *vs* 11.06%, $p = 0.028$). Similarly, i-Foxp3$^+$ Tregs were more tend to be clustered in patients with SSR>0.9628 (cell density: mean 285.8 *vs* 464.8, $p = 0.033$; percentage: mean 6.68% *vs* 10.88%, $p = 0.002$). Additionally, we examined the aggregation and distribution of CD4$^+$ Foxp3$^+$ Tregs and CD8$^+$ Foxp3$^+$ Tregs, the two major Treg subpopulations. Notably, patients with SSR>0.9628 exhibited higher infiltration of CD4$^+$ Foxp3$^+$ Tregs in both stromal and intra-tumoral area (mean s-cell density and s-percentage: 169.7 *vs* 287.4 and 5.05% *vs* 8.03%, $p = 0.026$, $p = 0.03$, respectively; mean i-cell density and i-percentage: 68.01 *vs* 172.4 and 1.65% *vs* 4.01%, $p = 0.011$, $p = 0.012$, respectively). Similar phenomena were also observed in CD8$^+$ Foxp3$^+$ Tregs (mean s-cell density and s-percentage: 33.82 *vs* 80.37 and 0.99% *vs* 2.18%, $p = 0.021$, $p = 0.019$, respectively; mean i-cell density and i-percentage: 21.99 *vs* 96.6 and 0.53% *vs* 2.09%, $p = 0.012$, $p = 0.009$, respectively). (Fig. 3C–D).

In addition to the increasing number of immunosuppressive cells, overexpression of immunosuppressive checkpoints also contributes significantly to immunosuppression. Notably, several immunosuppressive checkpoint pathways are induced directly as a result of abnormal TME. PD-L1 is currently the extensively investigated and best available immune checkpoint. As such, we compared the expression of PD-L1 and discovered that patients with SSR>0.9628 had greater levels of PD-L1 expression (METABRIC: mean 5.457 *vs* 5.521, $p < 0.0001$; TCGA: mean 1.096 *vs* 1.682, $p < 0.0001$) (Fig. 3A–B). In these patients with SSR>0.9628, m-IHC results consistently revealed a greater percentage (mean 10.24% *vs* 27.39%, $p = 0.0001$) and density (mean 379.5 *vs* 893.8, $p = 0.0026$) of PD-L1(+) cells (Fig. 3E).

3.4. MYC CNV is involved in EAAs metabolic reprogramming in BC

Tumor cell metabolic reprogramming can be triggered by genomic changes. MYC copy number variations, a transcription factor involved in the regulation of cell proliferation and metabolism, were extremely prevalent in BC. CNVs amplification or gain was found in approximately 50–60% of BC samples (METABRIC:47.95%; TCGA:59.17%) (Fig. 4A). Interestingly, the SSR scores were associated with the CNV status of MYC. SSR scores were found to be considerably higher in patients with MYC amplification (METABRIC: mean 1.17 *vs* 0.97; TCGA: mean 17.73 *vs* 1.99, all $p < 0.0001$) or gain (METABRIC: mean 1.11 *vs* 0.97; TCGA: mean 6.86 *vs* 1.99, all $p < 0.0001$) (Fig. 4B–C). Further mechanistic investigations revealed that increasing MYC copy number resulted in elevated *SLC7A5* (Amp and Gain *vs* Dip: METABRIC: mean 8.98 and 8.62 *vs* 7.91; TCGA: mean 48.02 and 31.99 *vs* 14.33, all $p < 0.0001$), but downregulated *SLC7A8* (Amp and Gain *vs* Dip: METABRIC: mean 7.86 and 7.99 *vs* 8.27; TCGA: mean 19.37 and 25.0 *vs* 30.18, all $p < 0.001$) (Fig. 4D–E). Therefore, the increased SSR score could be due to a disproportion between *SLC7A5* and *SLC7A8*, which was generated by MYC amplification or gain.

4. Discussion

The characteristic of tumor cells is metabolic dysfunction. Tumor cells are forced to undergo metabolic reprogramming as a result of carcinogenic mutation and nutritional deficiency in TME. However, because of this metabolic change, tumors become overly dependent on some EAAs. This metabolic susceptibility enables the use of EAAs deprivation or targeted EAAs metabolic therapy. Recent research indicates that some EAAs (tryptophan, histidine, methionine, and branched-chain amino acids) are directly associated with tumor growth and treatment resistance [20–23]. Although these studies have not revolutionized the clinical treatment plan for tumors in a significant way, they may imply that individuals have become more interested in the therapeutic transformation of EAA metabolism. Targeting the metabolism of EAAs is a promising therapy option that is currently being investigated.

Amino acids are polar molecules, requiring the assistance of transport carriers for transmembrane transport. The principal transporter of essential amino acids into cells is the L-type amino acid, transporter family [24]. *SLC7A5* and *SLC7A8* are capable of transporting nearly all types of EAAs, and their structures and transport substrates are similar, allowing them to work together to absorb EAAs. Simultaneously, they have a competitive interaction because both *SLC7A5* and *SLC7A8* can perform amino acid transport functions only when combined with CD98/4f2hc to form a complex [25]. We observed that the distribution of the two transporters was significantly different in normal and malignant cells. For example, while *SLC7A8* is highly expressed in normal breast cells, *SLC7A5* transporters are more abundant in BC cells. This is because *SLC7A5* has a higher substrate affinity than *SLC7A8* and is not pH-dependent, allowing for competitive uptake of EAAs by tumor cells in an acidic microenvironment with low amino acid levels. BC cells exhibit an imbalance between SLC7A5 and SLC7A8 transporters to meet the nutritional requirements of tumor cell proliferation. In this study, we first tried to measure this proportionate imbalance by comparing two transporters, specifically the SSR score. Interestingly, our data also shows a significant correlation between SSR and EAAs levels and metabolic activity in BC cells, which cannot be explained by *SLC7A5* or

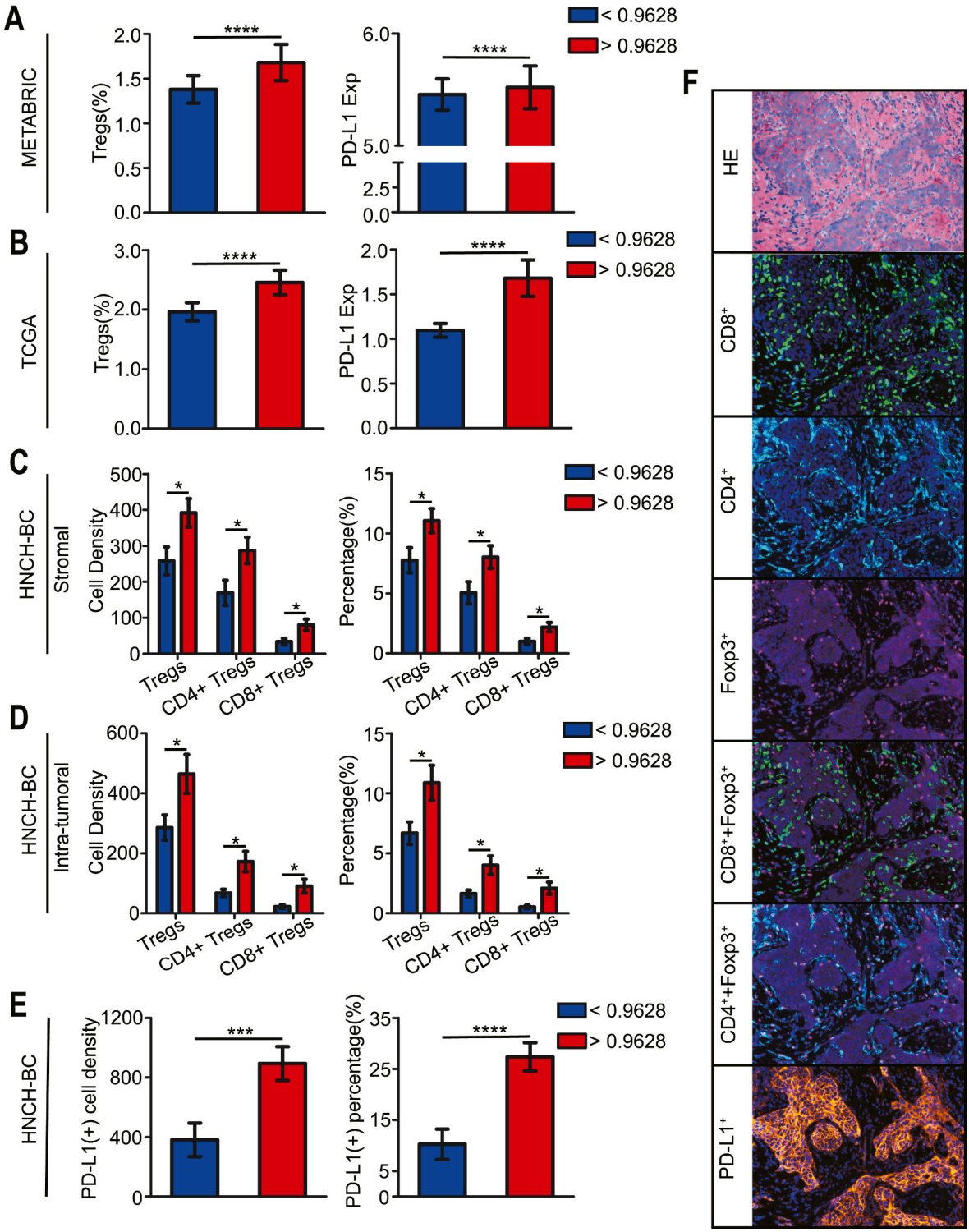

Fig. 3. Effects of EAAs metabolism on the immune microenvironment of BC, (A) Comparison of the infiltration of Tregs and the level of PD-L1 between BC patients with SSR>0.9628 and SSR< 0.9628 in METABRIC. (B) Comparison of the Tregs infiltration and level of PD-L1 between BC patients with SSR>0.9628 and SSR< 0.9628 in TCGA. (C) The density and percentage of stromal Tregs and main subpopulations of Tregs were compared between BC patients with SSR>0.9628 and SSR< 0.9628 in HNCH-BC. (D) The density and percentage of intra-tumoral Tregs and main subpopulations of Tregs were compared between BC patients with SSR>0.9628 and SSR< 0.9628 in HNCH-BC. (E) The density and percentage of PD-L1(+) cells were compared between BC patients with SSR>0.9628 and SSR<0.9628 in HNCH-BC. (Data indicated as mean ± SEM; * represents $p < 0.05$, ** represents $p < 0.01$, *** represents $p < 0.001$, **** represent for $p < 0.0001$) (F) Representative images of immunohistochemical (IHC) and multiplex immunohistochemical (m-IHC) staining of CD4, CD8, Foxp3, PD-L1, and composite images.

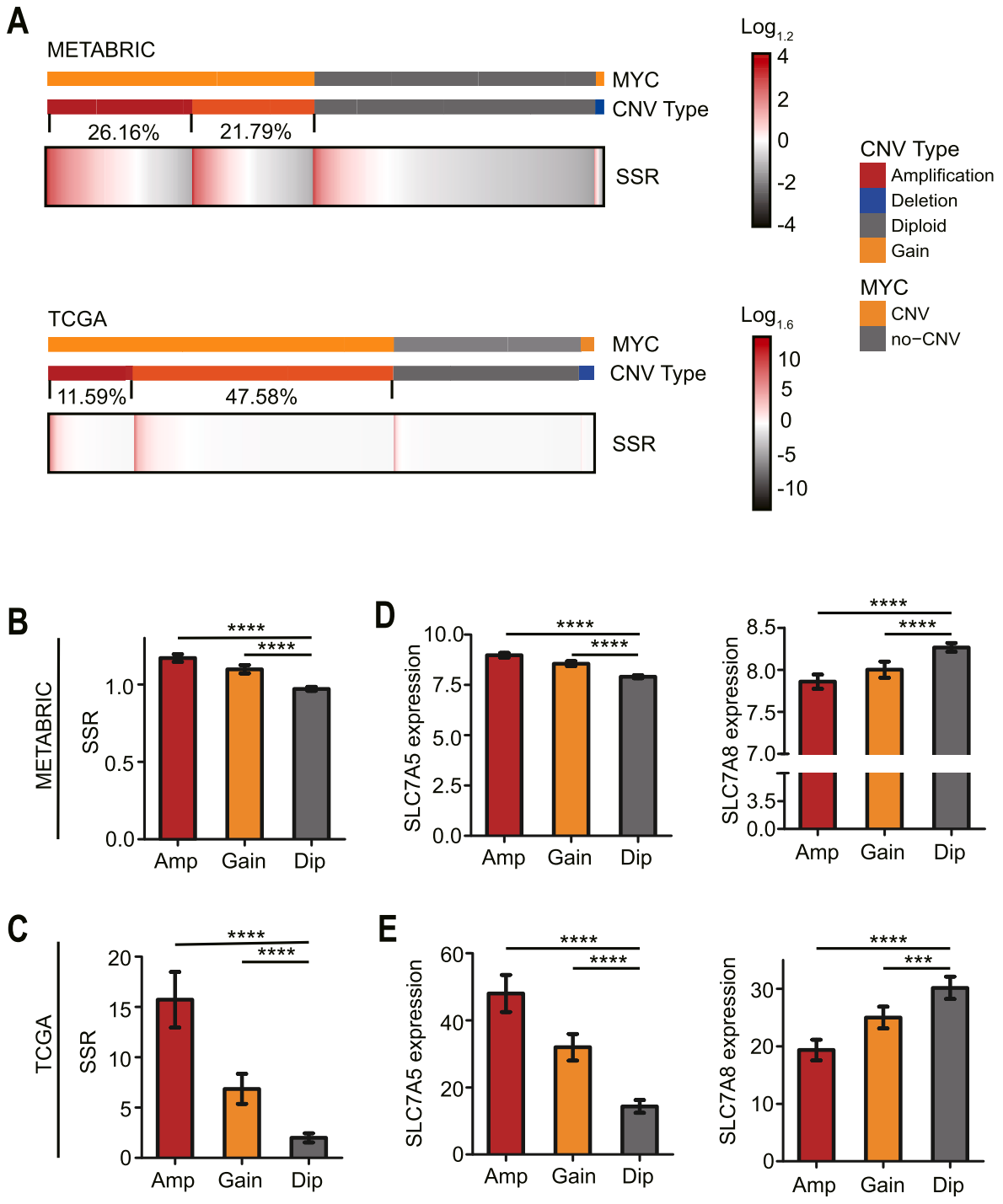

Fig. 4. MYC CNV is a molecular event of reprogramming of EAAs metabolism in BC, (A) Heatmaps represent the SSR scores of BC patients with various kinds of MYC CNV (Rows represent the SSR score, and columns indicate corresponding BC samples). Correlations between MYC CNV status and SSR scores of BC patients from METABRIC (B) and TCGA (C). Correlations between the MYC CNV status and the levels of gene expression for SLC7A5 and SLC7A8 in METABRIC (D) and TCGA (E). The Wilcoxon test was used to compare statistical differences, and the p values are labeled above each boxplot. Data is indicated as mean ± SEM; *** represents $p < 0.001$, **** represents $p < 0.0001$.

SLC7A8 alone. This discovery may result in the development of a novel, simple, and practical biomarker that can be used to estimate the level of EAAs in BC patients.

At present, few research has confirmed the relationship between EAA metabolism and the clinical prognosis of BC patients. However, abnormal EAAs metabolism has been associated with poor outcomes in a variety of cancers, which is consistent with the poor OS observed in BC patients with increased EAAs metabolism. As an independent risk factor for BC, high EAAs metabolism increases the prospect of targeting EAAs metabolism in the treatment of BC patients. In the meanwhile, tumor metabolic heterogeneity is an important factor to consider. Typically, previous research has administered metabolic inhibitors to patients in a non-specific manner. The efficacy of these drugs may be compromised if metabolic heterogeneity and dependency in tumors are ignored. Patients should be classified according to the level and degree of dependence on EAAs, safe and effective strategies for EAAs deprivation should be

developed based on their dependence and vulnerability on specific EAAs metabolism, because these strategies may be more beneficial to specific subpopulations of BC patients. Currently, the determination of tumor metabolic status is primarily based on mass spectrometry of tumor tissue and high-throughput sequencing of metabolism-related genes, but its widespread application is limited due to the complex nature and high cost. Accurate assessment of the EAAs metabolism of patients is the premise of precise implementation of deprivation treatment. Therefore, it is an essential concern to measure the EAAs metabolism of BC conveniently and efficiently. Our findings suggest a new and potentially useful indicator for measuring EAA metabolism in BC, but large-scale studies are needed to confirm its applicability.

Immunosuppression induced by metabolic competition between tumor cells and immune cells has been a research hotspot because immunotherapy has gradually become a more essential form of tumor treatment [26]. In the TME, both tumor cells and immune cells rely on EAAs to maintain metabolism and proliferation. The competitive uptake of EAAs by tumor cells significantly inhibits the immune response and killing function of immune cells. Bian et al. [18] recently discovered that the competitive uptake of methionine by tumor cells causes T cell apoptosis owing to malnutrition. Additionally, there is evidence that metabolic dysfunction of tumor cells results in the formation of an immunosuppressive microenvironment, with Treg cells serving as the primary component. It has been discovered that a decrease of leucine and elevation of tryptophan metabolites can cause $CD4^+$ T cells to differentiate into Treg cells [27]. Consistently, we observed that BC patients with a high EAAs metabolism had a higher infiltration of Treg cells and PD-L1 expression, implying that BC cancer's competitive uptake of EAAs promoted the formation of an immunosuppressive microenvironment. This finding contributes to our current understanding of the mechanism of immune escape induced by tumor metabolism. We can utilize the different metabolic needs between immune cells and tumor cells as the window of therapy to reverse immunosuppression.

The abnormal driving of oncogenes is commonly considered to be the cause of tumor metabolic reprogramming. Metabolic reprogramming may be based on molecular events involving key genes, such as gene mutation and copy number variation. MYC gene activation is primarily triggered by chromosome translocation or amplification, which can boost tumor cell growth and proliferation and play a vital regulatory function in metabolic reprogramming [28]. Importantly, we observed that the MYC gene amplification is a common molecular event in BC. This is interesting since MYC has previously demonstrated that it can promote EAA uptake by neuroblastoma cells via a positive feedback loop involving EAA-*MYC*-*SLC7A5* [29]. Similarly, we discovered that amplification of MYC in BC can result in an elevated SSR score, implying that MYC amplification may be a significant contributor to the imbalance of EAAs transporters. These evidences indicate that MYC may be a target for modulating the metabolic activity of EAAs in BC. Interestingly, we also detected that the downregulation of *SLC7A8* is involved in EAAs reprogramming of BC. Because there are very few research studies on *SLC7A8*, it is still unclear whether MYC amplification promotes *SLC7A8* downregulation. Overall, these findings raise some exciting questions and highlight an important direction for further research.

Many limitations and preliminary features exist in this investigation. First, we established for the first time that SSR is significantly correlated with the level of EAAs in BC cell lines and that SSR may partially reflect the metabolic activity of EAAs in BC patients. However, additional metabolomics, in vitro and in vivo functional testing are required to further verify and extend these results. Furthermore, we discovered that abnormally high EAAs metabolism increases immunosuppressive components in the BC TME; however, immunological testing is still needed to confirm and explain the specific mechanism of immune escape. Notably, this is the first report on the clinical utility of SSR in BC patients. The optimal SSR cut-off point (0.9628) was obtained from the study's enrolled BC patients. Although we used two approaches to verify that 0.9628 was the best and most stable cutoff value, the broad applicability of the cutoff point needs to be interpreted with caution and needs to be further confirmed and standardized in future prospective studies. Although this study has these limitations and preliminary properties, our findings provide new insights and directions for future research in the application of EAAs deprivation as a new treatment for BC patients.

5. Conclusion

In conclusion, we identified a novel biomarker for evaluating the EAA metabolic activity in BC and provide new evidence that enhanced EAA metabolism contributes significantly to poor prognosis and immunological suppression in BC. Additionally, we observed that MYC amplification is a potential molecular event to drive the metabolic reprogramming of EAAs in BC. These results have important clinical significance, but further validation in a larger patient cohort remains crucial.

Author contributions

Yajie Zhao and Chunrui Pu were responsible for the analysis, interpretation of data and graphing. Yajie Zhao wrote the manuscript. Zhenzhen Liu supervised the whole analysis and contributed to data analysis and editing of the manuscript. All authors contributed to the article and approved the submitted version.

Data availability statement

The data supporting the findings of this study are available within the article [and/or] its supplementary materials.

Funding statement

This research did not receive any specific grant from funding agencies in the public, commercial, or not-for-profit sectors.

Declaration of competing interest

The authors declare no potential conflicts of interest.

Acknowledgments

The results shown here are part based upon data generated by the TCGA Research Network: https://www.cancer.gov/tcga.

Appendix A. Supplementary data

Supplementary data to this article can be found online at https://doi.org/10.1016/j.breast.2022.02.009.

References

[1] Latest global cancer data: cancer burden rises to 19.3 million new cases and 10.0 million cancer deaths in 2020[J]. IARC; 2020.
[2] Brandon F, Ashley S, Deberardinis RJ. Metabolic reprogramming and cancer progression. Science 2020;368(6487):eaaw5473.
[3] Chowdhry S, Zanca C, Rajkumar U, et al. NAD metabolic dependency in cancer is shaped by gene amplification and enhancer remodelling. Nature 2019;569(7757):570–5.
[4] Du Siqi, Wang Yadi, Alatrash Nagham, et al. Altered profiles and metabolism of L- and D-amino acids in cultured human breast cancer cells vs. non-tumorigenic human breast epithelial cells. J Pharm Biomed Anal 2019;5(164):421–9.
[5] Lien EC, Ghisolfi L, Geck RC, et al. Oncogenic PI3K promotes methionine dependency in breast cancer cells through the cystine-glutamate antiporter xCT. Sci Signal 2017;10(510):eaao6604.
[6] Lu H, Chen I, Shimoda LA, et al. Chemotherapy-induced Ca^{2+} release stimulates breast cancer stem cell enrichment. Cell Rep 2021;34(1):108605.
[7] Strekalova E, Malin D, Weisenhorn E, et al. S-adenosylmethionine biosynthesis is a targetable metabolic vulnerability of cancer stem cells. Breast Cancer Res Treat 2019;175(1):39–50.

[8] Saito Y, Li L, Coyaud E, et al. LLGL2 rescues nutrient stress by promoting leucine uptake in ER+ breast cancer. Nature 2019;569(7755):275–9.
[9] Chen JY, Li CF, Kuo CC, et al. Cancer/stroma interplay via cyclooxygenase-2 and indoleamine 2,3-dioxygenase promotes breast cancer progression. Breast Cancer Res 2014;16(4):410.
[10] Soliman H, Rawal B, Fulp J, et al. Analysis of indoleamine 2-3 dioxygenase (Ido1) expression in breast cancer tissue by immunohistochemistry. Cancer Immunol Immunother 2013;62(5):829–37.
[11] Mansfield AS, Heikkila PS, Vaara AT, et al. Simultaneous Foxp3 and Ido expression is associated with sentinel lymph node metastases in breast cancer. BMC Cancer 2009;9:231.
[12] Butler M, Meer L, Leeuwen F. Amino acid depletion therapies: starving cancer cells to death. Trends Endocrinol Metabol 2021;32(6):367–81.
[13] Jeon H, Kim JH, Lee E, et al. Methionine deprivation suppresses triple-negative breast cancer metastasis in vitro and in vivo. Oncotarget 2016;7(41):67223–34.
[14] Strekalova E, Malin D, Good DM, et al. Methionine deprivation induces a targetable vulnerability in triple-negative breast cancer cells by enhancing TRAIL receptor-2 expression. Clin Cancer Res 2015;21(12):2780–91.
[15] Li H, Ning S, Ghandi M, et al. The landscape of cancer cell line metabolism. Nat Med 2019;25(5):850–60.
[16] Wang D, Wei G, Ma J, et al. Identification of the prognostic value of ferroptosis-related gene signature in breast cancer patients. BMC Cancer 2021;21(1):645.
[17] Zhao Y, Pu C, Liu Z. Exploration the significance of a novel immune-related gene signature in prognosis and immune microenvironment of breast cancer. Front Oncol 2020;10:1211.
[18] Jan B, Frederick K, Sinn BV, et al. Cutoff finder: a comprehensive and straightforward web application enabling rapid biomarker cutoff optimization. PLoS One 2012;7(12):e51862.
[19] Robert LC, Marisa DF, David LR, X-tile. A new bio-informatics tool for biomarker assessment and outcome-based cut-point optimization. Clin Cancer Res 2004;10 (21):7252–9.
[20] Bian YJ, Li W, Kremer DM, et al. Cancer SLC43A2 alters T cell methionine metabolism and histone methylation. Nature 2020;585(7824):277–82.
[21] Gao X, Sanderson SM, Dai Z, et al. Dietary methionine influences therapy in mouse cancer models and alters human metabolism. Nature 2019;572(7769):397–401.
[22] Kanarek N, Keys HR, Cantor JR, et al. Histidine catabolism is a major determinant of methotrexate sensitivity. Nature 2018;559(7715):632–6.
[23] Sadik A, Patterson L, Ztürk S, et al. IL4I1 is a metabolic immune checkpoint that activates the AHR and promotes tumor progression. Cell 2020;182(5):1252–70.
[24] Amo Eva M Del, Urtti A, Yliperttula M. Pharmacokinetic role of L-type amino acid transporters LAT1 and LAT2. Eur J Pharmaceut Sci 2008;35(3):161–74.
[25] Yan R, Zhao X, Lei J, et al. Structure of the human LAT1-4F2hc heteromeric amino acid transporter complex. Nature 2019;568(7750):127–30.
[26] Leone RD, Powell JD. Metabolism of immune cells in cancer. Nat Rev Cancer 2020; 20(9):516–31.
[27] Makowski L, Chaib M, Rathmell JC. Immunometabolism: from basic mechanisms to translation. Immunol Rev 2020;295(1):5–14.
[28] Dey P, Kimmelman AC, Depinho RA. Metabolic codependencies in the tumor microenvironment. Cancer Discov 2021;11(5):1067–81.
[29] Yue M, Jiang J, Gao P, Liu H, Qing G. Oncogenic MYC activates a feedforward regulatory loop promoting essential amino acid metabolism and tumorigenesis. Cell Rep 2017;12(2):3819–32.